New Catalytic Materials for the Direct Epoxidation of Propylene by Molecular Oxygen

Anusorn Seubsai, Michael Kahn, and Selim Senkan*[a]

The direct vapor-phase production of propylene oxide (PO) from propylene and molecular oxygen without the use of a co-reactant remains a challenging problem in industrial catalysis, in spite of several decades of research. Herein, the discovery of a new class of silica-supported multimetallic RuO_2–CuO_x–NaCl catalysts for the direct synthesis of PO from propylene and molecular oxygen is reported. This trimetallic catalyst exhibits durability and delivers PO selectivities of 40–50% at propylene conversions of 10–20% within 240-270 °C and at atmospheric pressure. The best performing catalysts are characterized by powder X-ray diffraction (PXRD) and transmission electron microscopy (TEM) and are determined to be composed of nanocrystalline domains of the three phases of RuO_2, CuO_x, and NaCl.

Introduction

Propylene oxide (PO) is an important and versatile intermediate used in the production of a large variety of valuable consumer products, such as polyurethane foams, polymers, propylene glycol, cosmetics, food emulsifiers, and as fumigants and insecticides.[1,2] Over 8 million tons of PO are produced annually from propylene.[1] Currently, the majority of the PO is produced by the chlorohydrin and peroxidation processes, both of which are besieged by the formation of significant amounts of coproducts, some of which also pose environmental hazards.[1,2] Recently, a process using H_2O_2 was also commercialized.[1,3] The disadvantage of the H_2O_2 process is the added cost of the hydrogen peroxide used. In short, direct synthesis of PO from propylene and oxygen remains an important goal in industrial catalysis.

The technology and the economical and environmental impacts of current, as well as alternate, propylene epoxidation processes were recently reviewed by Cavani and Teles[1] and by Nijhuis et al.[2] These reviews also provide excellent summaries of the earlier and current research into propylene epoxidation and, consequently, only a brief introduction will be provided here. Research into PO formation initially involved the use of Ag-based catalysts, in an attempt to reproduce the commercial success of ethylene oxide (EO) production.[1,2,4] However, these attempts were unsuccessful due to the presence of more reactive allylic hydrogen atoms in propylene, which led to the production of other C_3 products and CO_2. Other methods explored for PO synthesis have included the use of silica-supported Cu,[5] various single and mixed metal oxides,[6,7] Au-based catalysts with H_2[8] or H_2O[9] as co-reactants, titania-based catalysts,[10] molten salts of metal nitrates,[2] and the use of O_3[11] and nitrous oxide[2] as reactants. Although these developments are scientifically significant, they suffered from either low PO selectivities,[5–8] low propylene conversions,[5–8] or short catalyst lifetimes[10] or they required the use of higher pressures[7] or costly co-reactants.[2,11] Recently, Ag_3 clusters deposited on thin alumina film prepared by molecular beam techniques were also reported [Lei et al. 2010].[12] However, the scale-up of this catalytic material, prepared by molecular-beam techniques, and the prevention of the sintering of the Ag_3 clusters formed represent formidable challenges. It is important to note that PO yields similar to the results reported here were also seen in the homogeneous gas phase reactions of propylene and oxygen, that is, without a heterogeneous catalyst.[7] However, the high pressures (ca. 2.5 MPa) and the long reaction times (ca. 100 s) pose challenges for large-scale applications.

Consequently, the development of novel catalytic materials that enable the direct production of PO from propylene and molecular oxygen under atmospheric pressure remains an important technological challenge in heterogeneous catalysis.

The direct epoxidation of propylene by oxygen involves the following overall stoichiometry:

$$C_3H_6 + \tfrac{1}{2}O_2 \rightarrow C_3H_6O$$
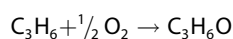
However, besides PO, the partial oxidation of propylene can also form a variety of byproducts, such as acetone (AT), acrolein (AC), acetaldehyde (AD), and propanal (PaL), together with deep oxidation products CO and CO_2. Previously, we explored the propylene epoxidation performances of 43 single metal or metal oxide catalysts supported on SiO_2 support using high-throughput catalysis tools and methods. These studies led to both confirmatory findings of catalysts for the epoxidation of propylene, such as Ag,[1,2,4] Cu,[5] and Pd,[10] and to the discovery of new leads, such as Bi, Ru, Cr, and Mn. Binary combinations of all of these lead metals subsequently led to the

[a] A. Seubsai, M. Kahn, Prof. Dr. S. Senkan
Department of Chemical Engineering, University of California
Los Angeles, CA 90095 (USA)
Fax: (+1) 310-440-8309
E-mail: ssenkan@gmail.com

determination of the bimetallic RuO_2–CuO_x/SiO_2 system as the most promising combination, albeit with low PO selectivities.

Herein we report the discovery of a new class of silica-supported multimetallic RuO_2–CuO_x–NaCl catalysts for the direct epoxidation of propylene by molecular oxygen under atmospheric pressure. This trimetallic catalyst exhibits PO selectivities of 40–50% at propylene conversions of 10–20% in the temperature range 240–270°C and at atmospheric pressure.

Results and Discussion

Before presenting the results, several issues must be stated. Firstly, the silica-supported Ru–Cu–Na trimetallic catalyst, RuO_2–CuO_x–NaCl, resulted in the production of PO as the primary C_3 product, with only small quantities of AC, AT, and AD. Other possible products, such as PaL, allyl alcohol and propionic acid, were not detected at all. In contrast, individual Ru and Cu catalysts, as well as their binary combinations, produced significant levels of AC and AT, a result consistent with earlier studies.[11] Secondly, CO_2 was the only deep oxidation product detected for the Ru–Cu–Na-catalyzed oxidation, with no detectable levels of CO formed.

PO selectivities and propylene conversions are presented for the Ru–Cu–Na/SiO_2 system in Figure 1 A and 1 B, respectively.

Propylene conversions (X_{PR}) were determined from the following:

$$X_{PR} = \{([PO]+[AC]+[AT]+2\,[AD]/3+[CO_2]/3)_{out}/[C_3H_6]_{in}\} \times 100\,\%$$

or

$$X_{PR} = \{([C_3H_6]_{in}-[C_3H_6]_{out})/[C_3H_6]_{in}\} \times 100\,\%$$

and selectivities to propylene oxide (S_{PO}) were then calculated using the following expression:

$$S_{PO} = \{([PO]/[PO]+[AC]+[AT]+2\,[AD]/3+[CO_2]/3)\} \times 100\,\%$$

The most remarkable aspect of these results (Figure 1) is that only the trimetallic combinations of Ru, Cu, and Na, that is, RuO_2–CuO_x–NaCl/SiO_2, exhibited the best PO selectivities (ca. 49%), with propylene conversions of 14%. In contrast, single and binary metal combinations exhibited poor epoxidation performances, consistent with previous studies.[5] For example, PO selectivity for CuO/SiO_2 was only 7% (i.e. the selectivity to CO_2 was 93%), with 0.6% conversion of propylene under the same experimental conditions. RuO_2/SiO_2 gave 11% propylene conversion but its PO selectivity was virtually nil. Silica-supported sodium was essentially an inert material for the reaction. Similarly, the performance of bimetallic catalytic materials was suboptimal. Sodium alone offered no promotional effect to Cu or to Ru. Although the Ru–Cu binary system gave up to 16% propylene conversion, the PO selectivity was only 14%. The optimal metal ratio in the trimetallic system was determined to be Ru/Cu/Na ≈ 4:2:1 metal weight ratio or 3:4:4 atomic ratio.
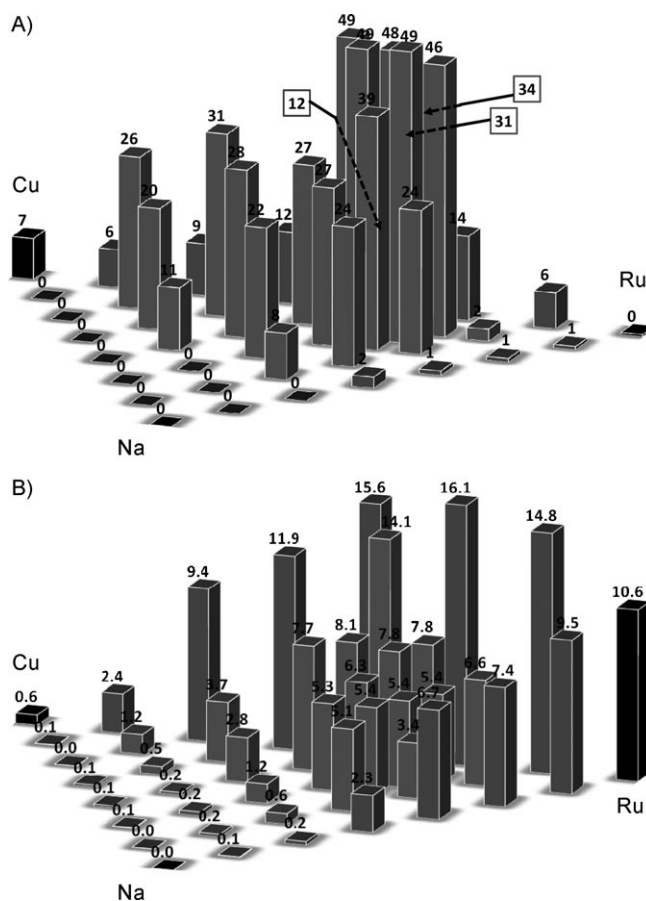

Figure 1. PO selectivities (A; values in squares refer to peaks that are hidden) and propylene conversions (B) as a function of Ru–Cu–Na concentrations (wt%) on the silica support. $T = 250$°C; feed-gas composition C_3H_6/O_2/He = 1:4:95; gas-hourly space velocity (GHSV) = 20 000 h^{-1}. Total metal loading was kept at 7% in these experiments to better compare the results. It is evident that higher PO selectivity catalysts were all trimetallic combinations, whereas single and bimetallic catalysts exhibited poor PO selectivities. Each corner of both diagrams represents the designated pure metal at 7 wt% loading.

In a recent computational study by Torres et al., the increased production of PO on Cu relative to Ag was attributed to the lower Lewis basicity of CuO_x,[14] which initially favors oxametallacycle formation followed by PO production. In contrast, the higher Lewis basicity of Ag_2O was shown to abstract an allylic H from propylene and form OH, which then leads to complete combustion. The participation of Cu_2O in propylene epoxidation was also suggested by others.[15] NaCl only in combination with Ru seems to create CuO_x sites with lower Lewis basicity, thus promoting oxametallacycle formation (Figure 1), provided the same mechanism remains valid in our trimetallic system.

The effects of NaCl, as seen on the kinetics of PO formation, are also in harmony with those reported for alkali metals and halogens for the case of EO formation catalyzed by Ag_2O.[16] For example, the highly electronegative Cl atoms embedded into the Cu clusters could weaken the Cu–O bond by withdrawing electrons from the surface Cu atoms, thereby improving PO selectivity. That is, the Cl effect is likely to be

electronic and not site-blocking, similar to Ag_2O surfaces.[16] Consequently, Cl would also affect the activation energy for the dissociative chemisorption of O_2 on CuO_x. In contrast, Na atoms are expected to occupy surface sites on Cu/CuO clusters, thus decreasing propylene conversion rates. However, depending on which sites are preferentially blocked (e.g. step sites), Na may improve PO selectivity. Clearly, additional experiments are required to better understand the individual effects of Na and Cl.

Changes in reaction temperature had the most pronounced impact on PO selectivities and propylene conversions (Figure 2); PO selectivity of about 65% can be achieved at
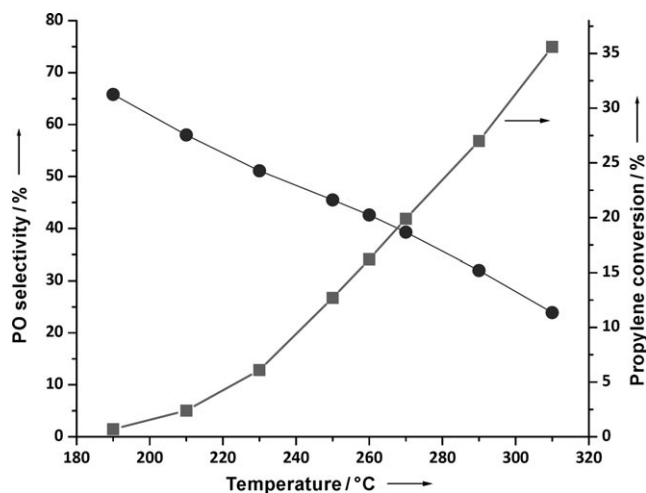

Figure 2. Increases in temperature significantly decrease PO selectivity (●) from 65% at 190 °C to 25% at 310 °C, whereas propylene conversion (■) increases to 36% over the same temperature range. However, within 240–260 °C the trimetallic Ru–Cu–Na catalysts delivered useful PO selectivities of 40–50% at significant propylene conversions of about 10–15%. Ru/Cu/Na = 4:2:1; total metal loading = 12.5 wt%

190 °C, albeit at a lower propylene conversion, and decreased to about 40% at 270 °C, concomitant with a substantial increase in propylene conversion to about 20%. Furthermore, in the temperature range 240–270 °C, the PO selectivities remained in the range 40–50%, while propylene conversions were 10–22% (Figure 2). These results are encouraging as they demonstrate the potential utility of our trimetallic catalyst system for industrial considerations with modest improvements in selectivity and conversion. Notably, these results were again obtained without the use of H_2 as a coreactant.

The effects of residence time on PO selectivity and propylene conversion are presented in Figure 3. Increased gashourly space volume (GHSV) decreased propylene conversions significantly, whereas it had a lesser impact on PO selectivity, especially at high space velocities. These findings suggest that, with improved catalyst and reactor designs, further increases in PO selectivities and propylene conversions should be possible.

In an attempt to further optimize the performance of the trimetallic Ru–Cu–Na/SiO$_2$ catalysts for PO synthesis, experiments were also performed to investigate the effects of total metal
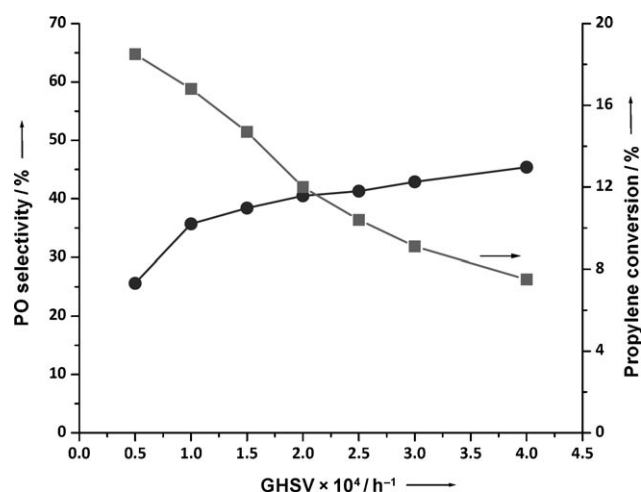

Figure 3. Effects of space velocity on PO selectivity (●) and propylene conversion (■). Higher space velocities slightly improve PO selectivity while decreasing propylene conversions. $T = 250$ °C, Ru/Cu/Na = 4:2:1; total metal loading = 8 wt%
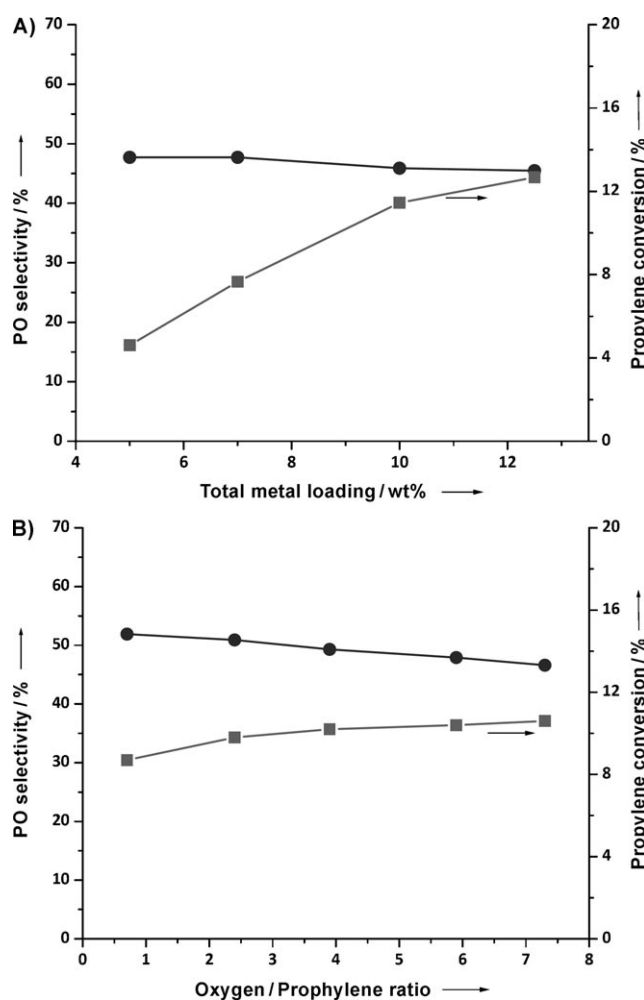
Figure 4. Increases in metal loading (Figure 4 A) slightly decrease PO selectivities (●) but significantly increase propylene conversions (■). In contrast, the effects of O_2/C_3H_6 ratio (Figure 4 B-Right) on PO selectivity and propylene conversion are minimal. $T = 250$ °C, GHSV = 20 000 h^{-1}, Ru/Cu/Na = 4:2:1.

loading and the feed gas composition (O_2/C_3H_6 ratio) at 250 °C and a GHSV of 20 000 h^{-1} (Figures 4 A and 4 B, respectively). Increasing the total metal loading from 5 wt % to 12.5 wt %
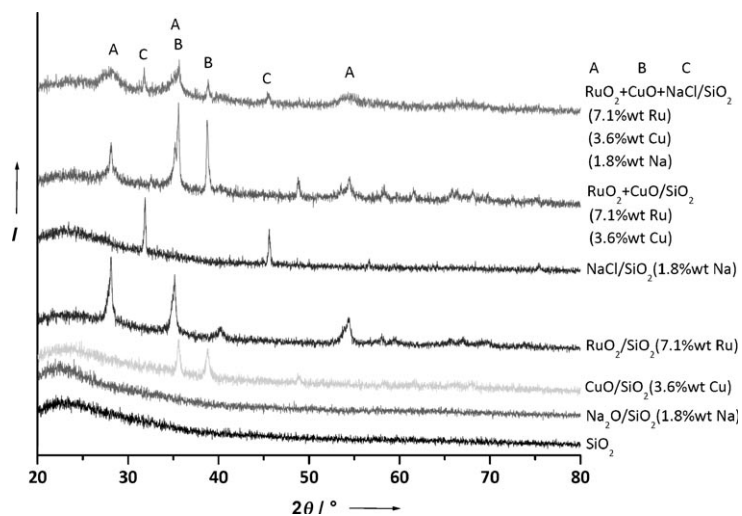
Figure 5. PXRD spectra of the SiO$_2$ support, RuO$_2$/SiO$_2$, CuO/SiO$_2$, and NaCl/SiO$_2$, as well as the bimetallic and trimetallic catalysts show the presence of distinct RuO$_2$ (A), CuO (B) and NaCl (C) phases. Loadings examined on SiO$_2$: Na$_2$O (1.8 wt % Na) prepared from NaNO$_3$, CuO (3.6 wt % Cu) prepared from Cu(NO$_3$)$_2$, RuO$_2$ (7.2 wt % Ru) prepared from [(NH$_4$)$_2$RuCl$_6$], NaCl (1.8 wt % Na) prepared from NaCl, bimetallic RuO$_2$+CuO, and trimetallic RuO$_2$+CuO+NaCl at identical metal loadings prepared from the same precursors and NaNO$_3$ as the sodium source.

decreased the PO selectivity slightly from 48 % to 43 %, while increasing the propylene conversion significantly from 4 % to 12 % (Figure 4 A). In contrast, increasing the O_2/C_3H_6 ratio from 0.5 to 7 decreased PO selectivity from 41 % to 35 %, while slightly increasing propylene conversion from 10 % to 12.5 % (Figure 4 B).

Powder X-ray diffraction (PXRD) spectra of the optimal trimetallic Ru–Cu–Na/SiO$_2$ catalysts together with those of the silica support and separately prepared RuO$_2$/SiO$_2$, CuO/SiO$_2$, RuO$_2$–CuO/SiO$_2$, Na$_2$O/SiO$_2$ (prepared from NaNO$_3$), and NaCl/SiO$_2$ are presented in Figure 5. The optimal trimetallic catalyst clearly incorporates distinct phases of RuO$_2$, CuO, and NaCl. The sodium precursor in this sample was NaNO$_3$, so the ruthenium precursor [(NH$_4$)$_2$RuCl$_6$] must have been the source of chlorine in NaCl. The preparation of trimetallic catalysts by sequential impregnation–drying–calcining steps resulted in poor epoxidation kinetics concomitant with the absence of the NaCl peaks in the PXRD spectra. Evidently NaCl promotion was key in the increased production of PO in our experiments. In addition, there was no sign of any chlorides on the RuO$_2$ spectrum despite the chlorine in the precursor, owing to the stability of the RuO$_2$ phase.

Compared to the single-component spectra for NaCl, RuO$_2$, and CuO, the spectrum for the trimetallic species displays a significant shortening and broadening of peaks, corresponding to a decrease in the mean crystallite dimensions. Based on the Scherrer equation,[17] the RuO$_2$ mean crystallite dimension decreased from approximately 37 nm in the single-component

sample to 12 nm in the trimetallic sample, whereas the CuO crystal dimension was virtually unchanged at 40 nm, and the NaCl dimension decreased from over 100 nm to approximately 90 nm. This latter finding indicates that sodium, in addition to the site-blockage effects noted earlier, could also be creating defects and crystal grain boundaries, thus aiding in the formation of a thermally stable lattice that contains finely tuned adsorption sites for the epoxidation of propylene. Additionally, by decreasing the crystallite dimensions, expensive catalytic materials are better utilized through improved dispersion.

The XRD findings are supported by limited transmission electron microscopy (TEM) studies. For example, the TEM image of fresh SiO$_2$-supported RuO$_2$–CuO–NaCl catalyst is shown in Figure 6. The amorphous fumed silica particles are of the order of 10 nm in diameter and appear aggregated. Metal clusters were also aggregated, exhibiting filamentous features with approximate dimensions of 10 nm × 30 nm. These filaments are likely be RuO$_2$ crystals, which are known to adopt tetragonal rutile crystal structures.[17] Further characterization work is clearly required to develop a better understanding of the structure of these trimetallic catalytic materials and to improve their catalytic performances.

Catalyst durability is essential for the practical utilization of newly discovered catalysts. Consequently, time-on-stream performance tests were also performed. The PO selectivities and propylene conversions over 6 h of continuous operation at 250 °C and 265 °C are shown in Figure 7 for the catalyst with the optimal composition, that is,
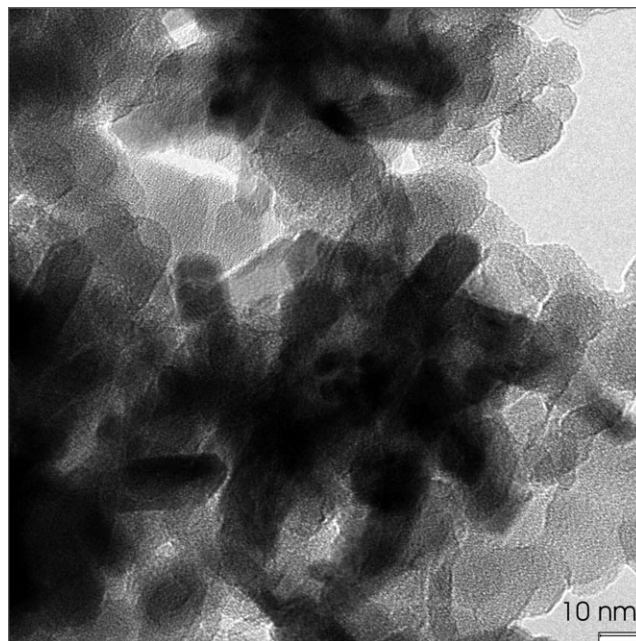
Figure 6. TEM image of the fumed SiO$_2$-supported RuO$_2$–CuO–NaCl catalyst. The scale bar is 10 nm. The amorphous fumed silica particles are indicated by light spheres and metal clusters are indicated by darker zones.
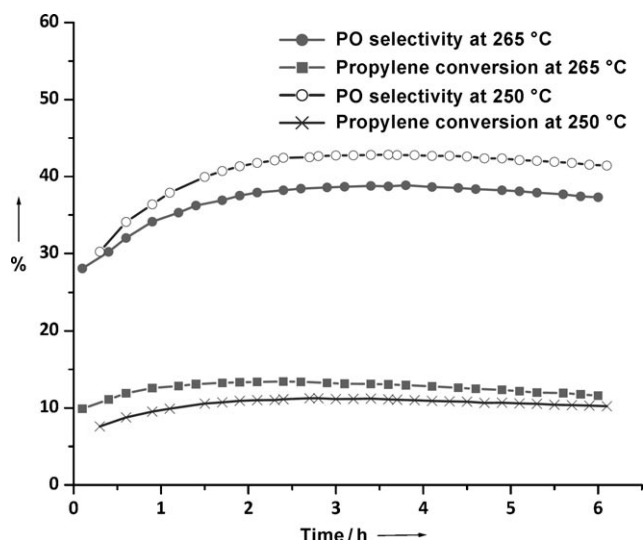
Figure 7. Time-on-stream testing results of the trimetallic Ru–Cu–Na/SiO$_2$ catalysts at 250 °C and 265 °C. Feed-gas composition C$_3$H$_6$/O$_2$/He = 1:4:95; GHSV = 20 000 h^{-1}. These findings clearly show the practical utility of these catalytic materials within the range of conditions investigated.

Ru/Cu/Na = 4:2:1. Evidently, the performance of the Ru–Cu–Na/SiO$_2$ catalysts actually improved during the first 2 h and remained at those levels for the entire 6 h testing period (Figure 7). PXRD spectra of these catalysts obtained after 0 h (fresh catalyst), 2 h, 4 h, and 6 h were also virtually identical, further supporting the time-on-stream data presented in Figure 7 that the catalyst remained unchanged after the testing period. The BET surface areas decreased slightly from about 174 m^{2}g^{-1} (fresh catalyst) to about 155 m^{2}g^{-1} after 6 h. However, no carbon (coke) deposition was detected at the end of the experiments.

In summary, trimetallic RuO$_2$–CuO–NaCl/SiO$_2$ catalysts gave useful PO selectivities in the range of 40–50 % and at propylene conversions of 10–20 % in the temperature range 240–270 °C and at atmospheric pressure. Such promising findings suggest that this catalytic system might be significant for further exploration and improvement. Our results are also in agreement with related investigations on EO synthesis regarding the promotion effects of alkali metals and halogens.

Experimental Section

The catalytic materials were all prepared by parallel co-impregnation of predetermined weights of amorphous fumed silica powder (SiO$_2$, Alfa Aesar, surface area 145 m^{2}g^{-1}) with aqueous solution mixtures of Ru ([(NH$_4$)$_2$RuCl$_6$], Aldrich), Cu [Cu(NO$_3$)$_2$, Alfa Aesar, ACS, 98.0%–102.0%], and/or Na [NaNO$_3$, Alfa Aesar, ACS, 99.0% min]. Different volumes and metal concentrations of the salt solutions were used to impart the desired and systematic variations of metal ratios and total metal loadings of the silica support. Each metal salt solution was then allowed to impregnate the support for 24 h in air. The resulting materials were then heated at 150 °C until dry, and calcined at 500 °C for 12 h in air. Therefore, the catalytic materials produced were expected to be either metal oxides or chlorides. When [(NH$_4$)$_2$RuCl$_6$] was used, NaCl was formed as the

solid-state product. Catalysts prepared by sequential impregnations exhibited poor epoxidation kinetics, most likely as a result of the lack of formation of NaCl, as discussed below. For the trimetallic Ru–Cu–Na system, firstly 36 distinct catalytic materials were prepared at 7 wt% total metal loading of the silica support, in 1 wt% increments. Once multimetallic compositions with superior PO selectivities had been determined, additional materials were synthesized using smaller composition increments to better identify the optimum Ru–Cu–Na ratio that results in maximum PO selectivity at useful propylene conversions. Once the optimal Ru–Cu–Na ratio was identified, the effects of total metal loading were also explored.

Catalyst characterizations were performed by powder X-ray diffraction (PANalytical X'Pert PRO fitted with Ni filter and Soller slit collimator). The Cu$_{K\alpha}$ radiation, at 45 kV and 40 mA was used to identify the active catalyst phases. BET surface areas were determined using Quantachrome Autosorb-1 units each with micropore analysis option.

Catalyst evaluations were performed using our computer-controlled array channel microreactor system, which is described elsewhere.[13] Reaction gases are flowed over the flat surfaces of compacted powders (5 mg) of catalytic materials that have been placed into wells along each reactor channel. This flow regime gives identical contact times in each channel, thereby enabling the direct comparison of the catalytic materials in a rapid fashion. The system allows the parallel screening of up to 80 catalyst samples. However, the actual number typically tested was less because duplicates and blank sites were used for improved quantification. All the experiments were carried out at temperatures in the range 190–310 °C, under atmospheric pressure and at GHSV values of 5000–40 000 h^{-1}. The feed gas consisted of propylene (C$_3$H$_6$; 1 vol%; Matheson, 99% purity) and O$_2$ (1–7 vol%; Matheson, 99.9%) with the balance of He (Matheson, 99.99%). Gas sampling was carried out by withdrawing reactor exit gases using a passivated 200 μm i.d. capillary sampling probe that was positioned within the reactor channel, monitored by on-line gas analysis by micro-GC (Varian, CP-4900) equipped with a thermal conductivity detector (TCD; 10 m, Porapak U) and molecular sieve 13X (10 m) columns. The propylene conversions, product selectivities, and product yields (calculated as product selectivity × propylene conversion) were calculated on the basis of carbon balances. GC calibrations for propylene, oxygen, and CO$_2$ were performed using mass flow controllers (MKS) with He as a carrier gas. Calibrations for PO, AC, AT, and AD were performed by vaporizing known quantities of liquid in a heated, evacuated 2250 cm^3 stainless steel tank and using He as a carrier gas. All calibrations yielded linear 5-point curves with $R^2 \geq 0.995$, using peak area as the basis for GC calculations. Reproducibility of the experiments was well within ±10%.

[1] F. Cavani, J. H. Teles, *ChemSusChem* **2009**, *2*, 508.
[2] T. A. Nijhuis, S. Musch, M. Makkee, J. A. Moulijn, *Appl. Catal. A* **2000**, *196*, 217.

[3] *Chem. Eng. News* **2006**, *84*, 22.

[4] J. R. Monnier, *Appl. Catal. A* **2001**, *221*, 73.

[5] O. P. H. Vaughan, G. Kyriakou, N. Macleod, M. Tikhov, R. M. Lambert, *J. Catal.* **2005**, *236*, 401.

[6] Z. X. Song, N. Mimura, J. J. Bravo-Suarez, T. Akita, S. Tsubota, S. T. Oyama, *Appl. Catal. A* **2007**, *316*, 142.

[7] H. Orzesek, R. P. Schulz, U. Dingerdissen, W. F. Maier, *Chem. Eng. Technol.* **1999**, *22*, 691.

[8] a) T. Hayashi, L. B. Han, S. Tsubota, M. Haruta, *Ind. Eng. Chem. Res.* **1995**, *34*, 2298; b) T. Hayashi, K. Tanaka, M. Haruta, *J. Catal.* **1998**, *178*, 566; c) B. S. Uphade, M. Okumura, S. Tsubota, M. Haruta, *Appl. Catal. A* **2000**, *190*, 43; d) A. K. Sinha, S. Seelan, S. Tsubota, M. Haruta, *Angew. Chem.* **2004**, *116*, 1572–1574; *Angew. Chem. Int. Ed.* **2004**, *43*, 1546.

[9] J. H. Huang, T. Akita, J. Faye, T. Fujitani, T. Takei, M. Haruta, *Angew. Chem.* **2009**, *121*, 8002–8006; *Angew. Chem. Int. Ed.* **2009**, *48*, 7862.

[10] a) K. Murata, Y. Kiyozumi, *Chem. Commun.* **2001**, 1356; b) K. Murata, Y. Liu, N. Mimura, M. Inaba, *Catal. Commun.* **2003**, *4*, 385.

[11] T. Berndt, and S. Brasel, *Chem. Eng. Technol.* **2009**, *32*, 1189.

[12] Y. Lei, F. Mehmood, S. Lee, J. Greeley, B. Lee, S. Seifert, R. E. Winans, J. W. Elam, R. J. Meyer, P. C. Redfern, D. Teschner, R. Schlögl, M. J. Pellin, L. A. Curtiss, S. Vajda, *Science* **2010**, *328*, 224.

[13] a) S. Senkan, K. Krantz, S. Ozturk, V. Zengin, I. Onal, *Angew. Chem.* **1999**, *111*, 867; *Angew. Chem. Int. Ed.* **1999**, *38*, 791; b) S. M. Senkan, S. Ozturk, *Angew. Chem.* **1999**, *111*, 2965; *Angew. Chem. Int. Ed.* **1999**, *38*, 2794.

[14] D. Torres, N. Lopez, F. Illas, R. M. Lambert, *Angew. Chem.* **2007**, *119*, 2101; *Angew. Chem. Int. Ed.* **2007**, *46*, 2055.

[15] W. M. Zhu, Q. H. Zhang, Y. Wang, *J. Phys. Chem. C* **2008**, *112*, 7731.

[16] K. C. Waugh, M. Hague, Ch. 7 in *Mechanisms in Homogeneous and Heterogeneous Epoxidation Catalysis* (Ed.: S. T. Oyama), Elsevier, Amsterdam, NL **2008**, pp. 85–110.

[17] R. W. G. Wyckoff, *Crystal Structures*, Wiley, New York, **1963**.